



OPEN

Multi enzyme production and alginate encapsulation from *Bacillus subtilis* for stable feed additives

Hamza Rafeeq¹✉, Muhammad Anjum Zia¹✉, Muhammad Shahid¹ & Muhammad Sarwar Khan²

Microbial enzymes improve feed digestibility but face challenges of high cost and low stability. In this study, we optimized the production of protease, lipase, cellulase, and amylase from *Bacillus subtilis* using response surface methodology. We purified the enzymes and encapsulated them in alginate beads to enhance performance. Encapsulation widened their active pH and temperature ranges. It also improved storage stability, with encapsulated enzymes retaining 60–74% activity after 30 days at 4 °C compared to 34–42% for free enzymes. These results show that alginate encapsulation increases enzyme robustness under variable conditions. The novelty of this work lies in the simultaneous optimization of four enzymes from one strain and their stabilization using a simple food-grade carrier. While the study demonstrates strong *in vitro* potential for poultry feed enrichment, *in vivo* trials are required to confirm practical application.

Keywords *Bacillus subtilis*, Optimization, Response surface methodology, Characterization, Encapsulation, Alginate, Poultry feed premix, Enzyme stabilization

It is widely acknowledged that microorganisms are essential for the industrial production of intracellular and extracellular enzymes¹. Products like cheese, bread, wine, and beer may be made from chosen organisms that are cultivated in fermenters under ideal circumstances to achieve maximum production^{2,3}. According to Ding et al.⁴ enzymes play a crucial role in the majority of cellular processes by acting as catalysts. The fact that microbial enzymes may be mass-produced using well-established fermentation procedures is a huge advantage. Microbes tightly regulate enzyme synthesis, making it possible to manipulate and leverage these regulatory mechanisms to enhance enzyme productivity⁵.

Bacillus species typically produce extracellular enzymes, with *Bacillus subtilis* being a common producer in industrial settings. Akinsemolu et al.⁶ and Liu and Kokare⁷ state that only a small number of the enzymes derived from microbes are suitable for commercial production, with the exception of proteases, lipases, cellulases, amylases, and xylanases. Soil is the primary habitat for *B. subtilis*, also known as the hay bacillus or grass bacillus. According to Shi et al.⁸ this organism, which has a rod-shaped body, has the ability to produce a durable endospore that protects itself from harsh environments. Both non-pathogenic and pathogenic *Bacillus* species are obligate aerobes or facultative anaerobes⁹.

Optimizing the economic and operational efficiency of a bioprocess begins with optimizing the process conditions. One variable-at-a-time (OVAT), the traditional optimization approach, may be effective in some situations¹⁰. By keeping all other variables constant, this technique allows one independent variable to fluctuate. The old approach requires numerous trials, which can be challenging and time-consuming. This approach disregards the potential effects of variable interactions¹¹. The response surface methodology is a statistical technique-based approach that allows for the identification of many variable interactions in a small number of tests. Abdollahzadeh et al.¹² use the RSM approach in optimization to achieve the optimal result as quickly as possible, while simultaneously studying the interactions of other variables. This technology enables the customization of media and growth conditions for cultivating various compounds, including enzymes, ethanol, amino acids, and primary and secondary metabolites¹³. Kumar et al.¹⁴ also use it to optimize the production of enzymes such as protopectinase, pectinase, cellulolytic, and xylanase.

¹Department of Biochemistry, University of Agriculture Faisalabad, Faisalabad 38040, Punjab, Pakistan. ²Centre of Agricultural Biochemistry and Biotechnology (CABB), University of Agriculture, Faisalabad 38040, Pakistan. ✉email: Butt.hamza2014@gmail.com; anjum.zia@uaf.edu.pk

Poultry feeds often contain indigestible components such as complex carbohydrates, cellulose, and proteins bound to anti-nutritional factors, which reduce nutrient availability and feed efficiency^{5,8}. To overcome these limitations, exogenous enzymes are routinely added to poultry diets, as they improve digestibility and nutrient absorption. However, current commercial enzyme products face two major challenges: they are expensive to produce and exhibit poor stability under storage and high-temperature pelleting conditions. Moreover, most studies have focused on single-enzyme supplementation^{19–22}, while poultry feed requires a synergistic mix of multiple enzymes for maximum efficiency.

The novelty of this work lies in the simultaneous optimization of four major hydrolytic enzymes (protease, lipase, cellulase, and amylase) from a single *Bacillus subtilis* strain using RSM and their subsequent encapsulation in alginate beads for improved stability. Unlike prior studies that focused on optimizing or encapsulating individual enzymes, the present work uniquely combines four hydrolytic enzymes, protease, lipase, cellulase, and amylase, produced by a single *Bacillus subtilis* strain. This integrated optimization and encapsulation strategy offers a unified platform for developing enzyme premixes suitable for poultry feed applications. Such a multi-enzyme encapsulation approach enhances potential synergism and practical relevance for complex feed substrates. The current study reports optimization, purification, encapsulation, and in vitro characterization of enzymes. An in vivo feeding trial was conducted, but it will be published separately. This manuscript focuses on the in vitro data to highlight the production process and encapsulation performance.

Results

Optimized production of enzymes

In the current study, various conditions of pH, temperature, incubation period, and inoculum size were optimized for fermentation media to produce protease, lipase, cellulase, and amylase from *Bacillus subtilis* (Supplementary Table 1). The results depicted that all enzymes (protease, lipase, cellulase, and amylase) showed maximum activities at pH 7. The optimum temperature for protease was found to be 25 °C, while lipase, cellulase, and amylase showed maximum activity at 40 °C. It was also found that protease and cellulase showed maximum activities at 72 h while lipase and amylase showed maximum activities at 48 h. Likewise, in the case of inoculum size, protease, lipase, and amylase showed maximum activities at an inoculum size of 3 mL, while cellulase showed maximum activity at 2 mL.

ANOVA for response surface quadratic model for protease

The ANOVA results confirmed that the RSM models were reliable for predicting enzyme production under different fermentation conditions (Supplementary Tables 2–10). For protease and amylase, the models showed high F-values and low p-values ($p < 0.05$), indicating that the selected factors significantly influenced enzyme activity. The high R^2 and adjusted R^2 values further demonstrated that the models explained most of the variation in the experimental data.

In contrast, the lipase and cellulase models showed lower predictive accuracy, as reflected by negative predicted R^2 values. This suggests that although the models could describe the observed data, their ability to predict new responses was limited. Such outcomes are often linked to biological variability or to interactions not fully captured in the design. We therefore interpreted the results of lipase and cellulase optimization with caution.

The 3D response surface plots for each enzyme further illustrate the influence of pH, temperature, incubation time, and inoculum size on enzyme activity (Figs. 1, 2, 3 and 4).

Enzyme purification

The purification of each enzyme was performed using ammonium sulfate precipitation, dialysis, and gel filtration techniques. During the purification process, the crude enzymes protease, lipase, cellulase, and amylase showed an overall activity of 6.25, 20.45, 85.76, and 9.02 U/mL and a specific activity of 1.29, 16.78, 7.11, and 13.4 IU/mg, respectively. Throughout each stage of the purification process, the overall activity of the enzymes declined, but the specific activity rose. The enzymes were partially purified via precipitation using 80% ammonium sulfate saturation. The enzymes (protease, lipase, cellulase, and amylase) obtained showed a specific activity of 13.7, 31.62, 14.68, and 28.5 IU/mg, respectively, and their purification increased up to 6.34, 5.0, 2.06, and 18.7-fold, respectively. Following three buffer changes during dialysis, the protease, lipase, cellulase, and amylase that had been partially purified showed a specific activity of 18.3, 39.08, 33.5, and 37.4 IU/mg, and purification increased up to 12.67, 7.63, 31.22, and 21.09 folds. The enzymes were then purified through Sepharose CL-6B gel filtration, which purified the enzymes (protease, lipase, cellulase, and amylase) up to 87.5, 42.6, 68.12, and 89.03 folds with specific activities of 26.4, 82.73, 85.3, and 56.2 IU/mg, respectively (Table 1).

Characterization

The purified enzymes were characterized through SDS-PAGE analysis. In Fig. 5 (a, c, and d), Lane-1 represents the marker protein, Lane-2 represents the crude enzyme, and Lane-3 represents the purified enzyme. In contrast, in Fig. 5(b), Lane-1 represents the marker proteins, Lane-2 represents the purified enzyme, and Lane-3 represents the crude enzyme. The molecular characterization of each enzyme indicates that the molecular weights of the protease, lipase, cellulase, and amylase isolated from *B. subtilis* were determined to be 29 kDa, 45 kDa, 45 kDa, and 56 kDa, respectively (Fig. 5a-d).

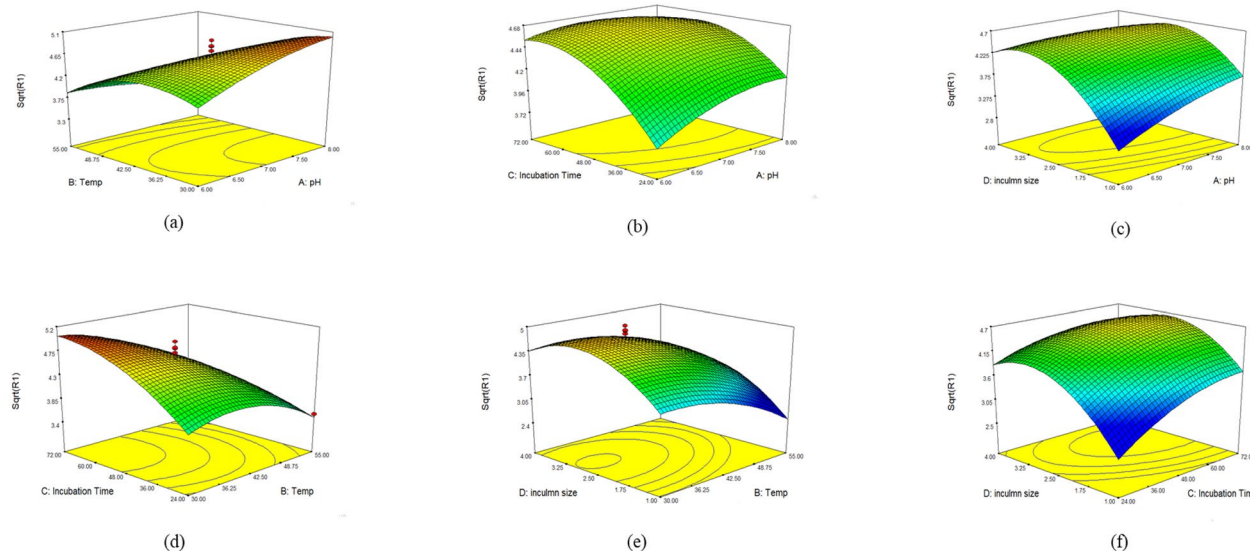


Fig. 1. Response surface plots showing the effect of fermentation parameters (pH, temperature, incubation time, and inoculum size) on the production of protease by *Bacillus subtilis*. Each axis represents one variable, and the response surface indicates predicted enzyme activity based on the RSM model.

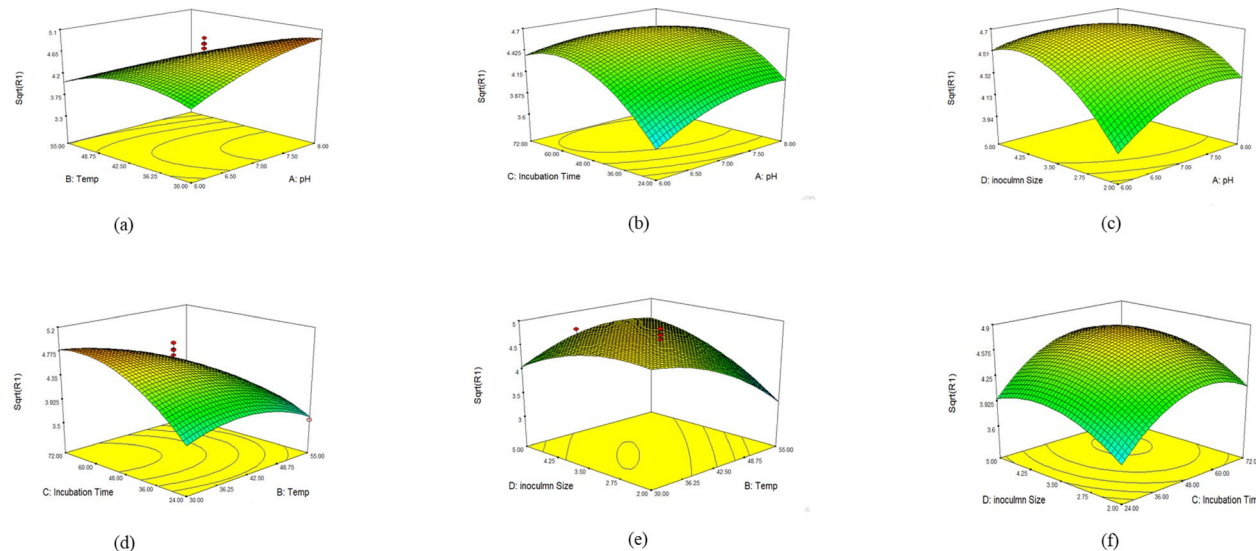


Fig. 2. Response surface plots showing the effect of fermentation parameters (pH, temperature, incubation time, and inoculum size) on the production of lipase by *Bacillus subtilis*. Each axis represents one variable, and the response surface indicates predicted enzyme activity based on the RSM model.

Characterization of alginate coated enzymes

FTIR analysis

According to FTIR analysis, the alginate-coated amylase exhibited a peak at 1000 cm⁻¹, corresponding to the polysaccharide structure of alginate (C-O and C-O-C vibrations). 2nd peak at 1600 cm⁻¹ indicates the presence of the C=O stretching bond in carboxylate groups of alginate and N-H bending in amides present in amylase (Fig. 6a). The FTIR analysis of alginate-coated lipase showed maximum peaks at 500–1650 cm⁻¹ region. Here, the peaks between 800 and 1000 indicate the C-O-C stretching vibrations from alginate. Likewise, the peaks between 1150 and 1250 cm⁻¹ indicate C-O-C stretching in the ether present in alginate, while the peak at 1550 cm⁻¹ indicates the N-H bending and C-N stretching vibrations of lipase (Fig. 6b). The FTIR analysis of alginate-coated protease indicates a peak at 1000 cm⁻¹, which depicts the C-O-C stretching vibration of alginate. 2nd peak between 1400 and 1500 cm⁻¹ indicates the C-H bending from the methyl group present in alginate and protease (Fig. 6c). Likewise, the FTIR analysis of alginate-coated cellulase indicated a sharp peak at 1000 cm⁻¹, indicating the C-O-C stretching vibrations for alginate. The peak at 1100 cm⁻¹ indicates the glycosidic linkages

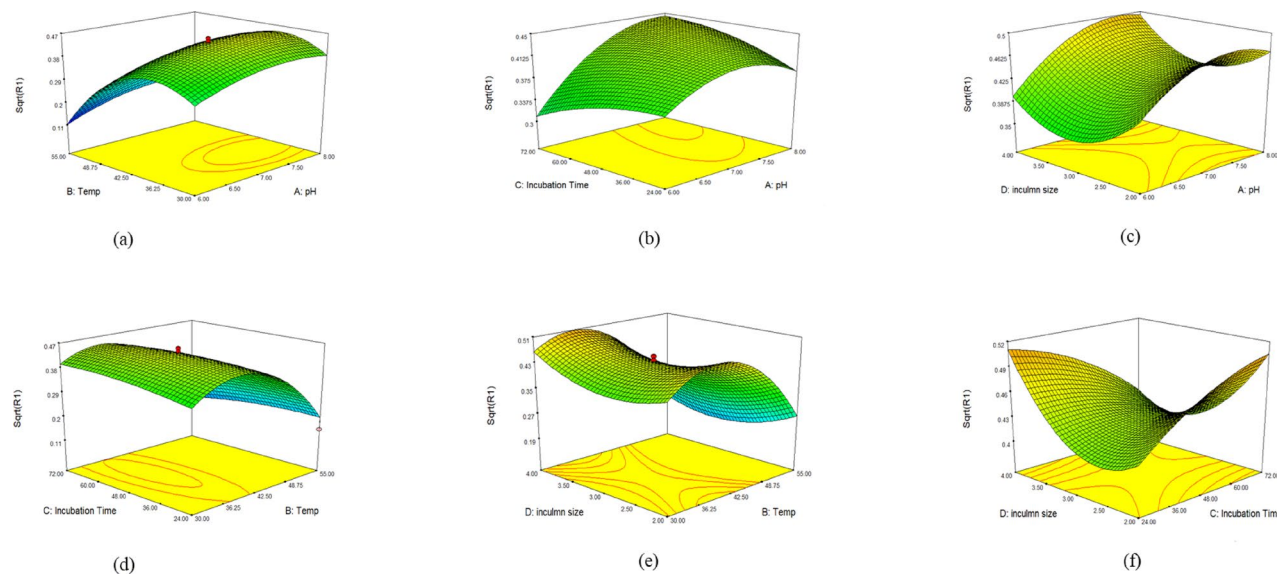


Fig. 3. Response surface plots showing the effect of fermentation parameters (pH, temperature, incubation time, and inoculum size) on the production of cellulase by *Bacillus subtilis*. Each axis represents one variable, and the response surface indicates predicted enzyme activity based on the RSM model.

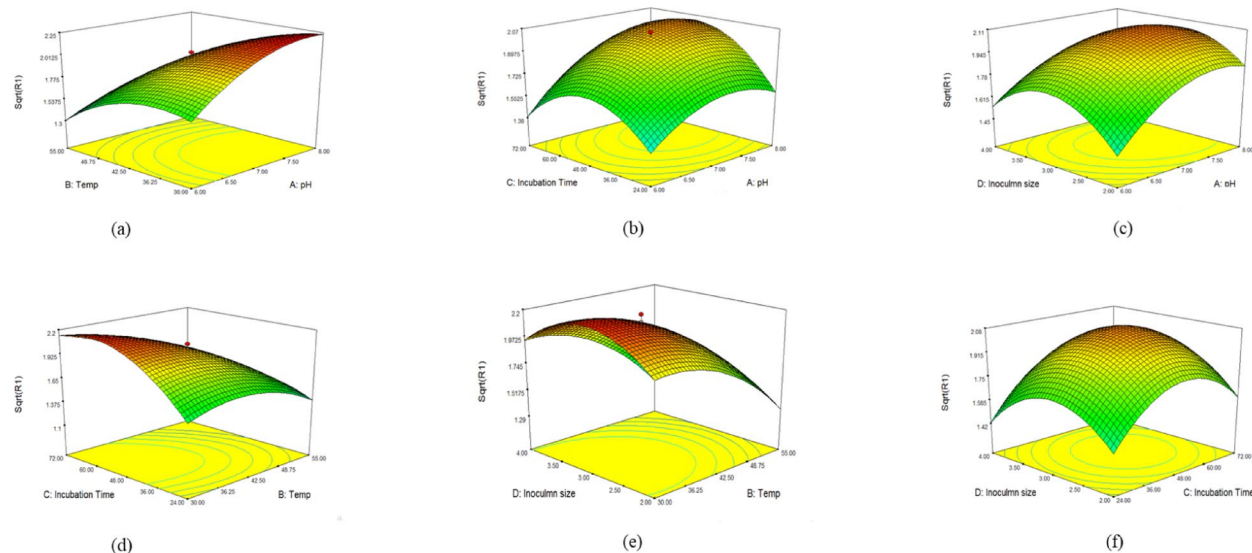


Fig. 4. Response surface plots showing the effect of fermentation parameters (pH, temperature, incubation time, and inoculum size) on the production of amylase by *Bacillus subtilis*. Each axis represents one variable, and the response surface indicates predicted enzyme activity based on the RSM model.

in alginate and cellulase. Likewise, a peak at 1600 cm⁻¹ indicates the presence of the C=O stretching bond in carboxylate groups of alginate and N-H bending in amides present in cellulase. A peak at 3300 cm⁻¹ indicates the potential hydrogen bonding between alginate and cellulase (Fig. 6d).

XRD analysis

Figure 7 depicts that the multiple peaks of each alginate-coated enzyme (amylase, lipase, protease, and cellulase) indicate that these alginate-coated enzymes have well-defined crystalline structures, which confirms the significant stability of each alginate-coated enzyme. Since the XRD analysis of alginate-coated enzymes showed sharp peaks, it indicates the presence of larger crystallites in solution.

Enzymes	Purification steps	Activity (U/mL)	Protein content (mg/mL)	Specific activity (IU/mg of protein)	Purification (fold)
Protease	Crude enzyme	6.25	4.84	1.29	1
	(NH ₄) ₂ SO ₄ precipitation	4.375	0.32	13.7	6.34
	Dialysis	3.187	0.17	18.3	12.67
	Sepharose CL-6B	2.125	0.08	26.4	87.5
Lipase	Crude enzyme	20.45	1.218	16.78	1
	(NH ₄) ₂ SO ₄ precipitation	14.29	0.45	31.62	5.9
	Dialysis	12.09	0.309	39.08	7.63
	Sepharose CL-6B	6.98	0.084	82.73	42.6
Cellulase	Crude enzyme	85.76	12.06	7.11	1
	(NH ₄) ₂ SO ₄ precipitation	27.98	1.905	14.68	2.06
	Dialysis	5.87	0.175	33.5	31.22
	Sepharose CL-6B	4.65	0.054	85.3	68.12
Amylase	Crude enzyme	9.02	0.673	13.4	1
	(NH ₄) ₂ SO ₄ precipitation	6.05	0.212	28.5	18.7
	Dialysis	5.67	0.151	37.4	21.09
	Sepharose CL-6B	1.63	0.029	56.2	89.03

Table 1. Summary of purification of enzymes at different steps.

Enzyme kinetics

Effect of temperature

Figure 8 represents the effect of temperature on the enzymatic activity (a) protease, (b) lipase, (c) cellulase, and (d) amylase (uncoated and encapsulated). Results depicted that in uncoated form, protease showed maximum activity at 50–60 °C, lipase at 40 °C, cellulase at 40–60 °C, and amylase at 50–60 °C. Results also depicted that protease, cellulase, and amylase showed reduced activities above 60 °C, while lipase showed reduced activities above 40 °C. But in encapsulated form, an increase in enzymatic activity of each enzyme was observed at each temperature range, and after encapsulation, protease, cellulase, and amylase showed maximum activity up to 70 °C. In contrast, lipase showed maximum activity up to 60 °C.

Effect of pH

Figure 9 represents the effect of pH on the enzymatic activity (a) protease, (b) lipase, (c) cellulase, and (d) amylase (uncoated and encapsulated). Results depicted that in uncoated form, protease showed maximum activity at pH 7–9, lipase at 7.5–8.5, cellulase at 6–7, and amylase at 6.5–7.5, and above that pH, these enzymes showed a reduction in their activities. But in encapsulated form, an increase in enzymatic activity of each enzyme was observed at each pH range, and after encapsulation, protease, lipase, cellulase, and amylase showed maximum activity at pH 5–10, 5.5–9.5, 4–9, and 4.5–9.5, respectively.

Stability

Residual activities of free and encapsulated enzymes were monitored at 4 °C for 30 days (Fig. 10). All enzymes showed a progressive decline in activity with time, but encapsulation markedly slowed this loss. Protease retained 74% of its initial activity after 30 days when encapsulated, whereas the free enzyme fell to 35%. Lipase displayed a similar trend, maintaining 67% activity in encapsulated form compared with 42% for the free enzyme at day 30. Encapsulated cellulase preserved 61% of its original activity after 30 days, while the free enzyme dropped to 34%. Encapsulated amylase retained 66% of its activity at day 30, in contrast to 39% for the free enzyme. These results demonstrate that alginate encapsulation substantially improves the storage stability of all four enzymes.

Discussion

The present study aimed to develop an enzyme premix for poultry feed by optimizing the production of protease, lipase, cellulase, and amylase from *Bacillus subtilis*. The combined optimization and encapsulation of multiple enzymes from a single strain represents a methodological advancement over previous single-enzyme studies. This design simplifies upstream fermentation and downstream formulation, potentially improving efficiency for industrial feed premix production. Members of the *Bacillus* genus are well known for producing antibiotics, enzymes, insecticides, and vitamins, and they are valued in industrial applications for their rapid growth and extracellular protein secretion^{15,16}. In this study, we optimized the fermentation conditions of pH, temperature, incubation period, and inoculum size to enhance enzyme yields. *Bacillus subtilis* secretes a variety of degradative enzymes¹⁷. Several proteins are generated during the exponential growth phase, but the bulk are made during the stationary phase that occurs before spore formation. Species from the *Bacillus* group can form spores, which allow them to withstand harsh environments and have beneficial effects in the host.

The optimized production of protease, lipase, cellulase and amylase through RSM indicated pH 7 an optimum pH for each enzyme, 25 °C an optimum temperature for protease and 40 °C for lipase, cellulase and amylase, 72 h incubation time an optimum time period for protease and cellulase while 48 h for lipase and amylase and 3 mL inoculum size for maximum production of protease, amylase and lipase while 2 mL for cellulase. These results

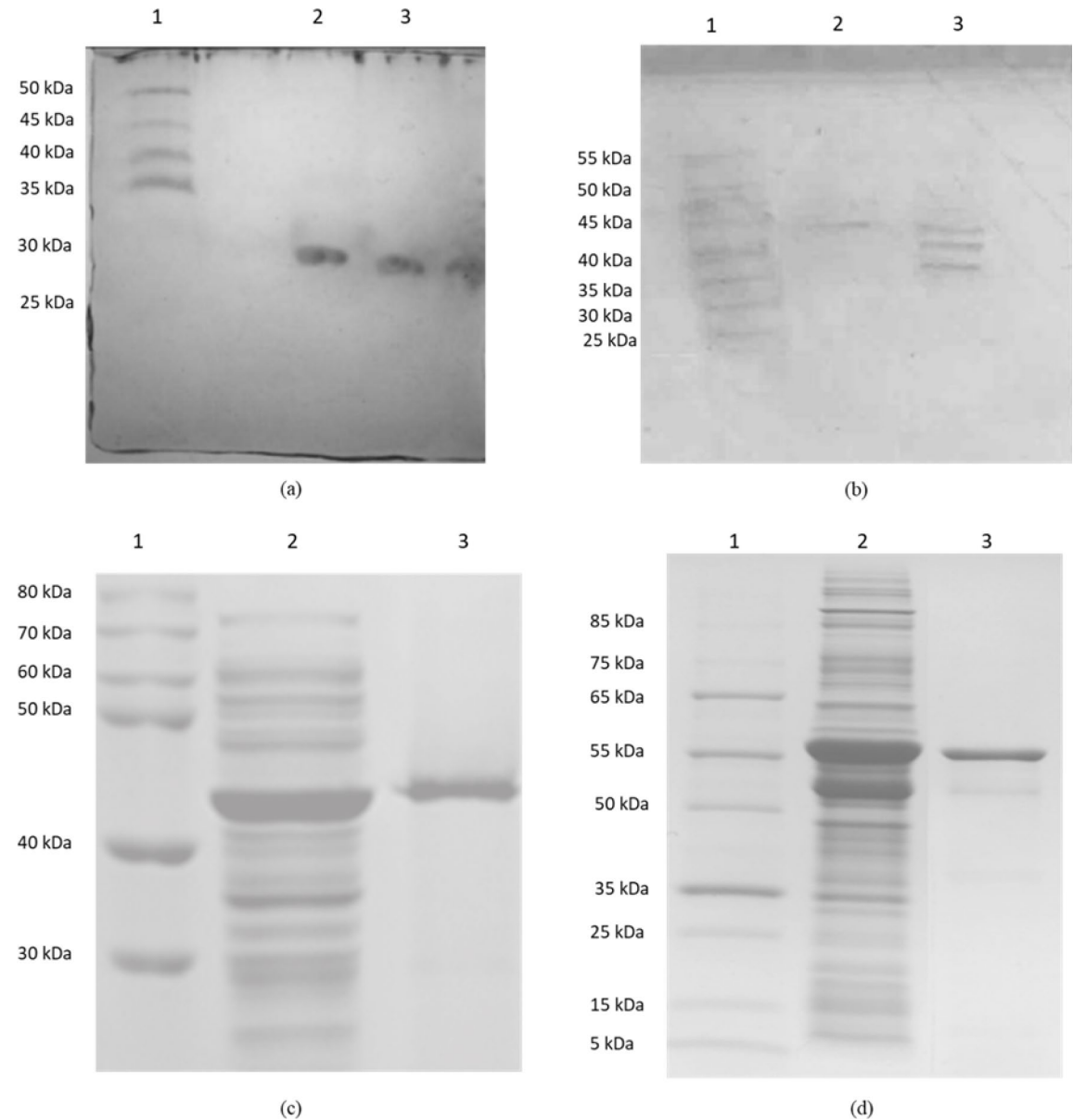


Fig. 5. Characterization of (a) protease, (b) lipase, (c) cellulase, and (d) amylase through SDS-PAGE analysis. (a, c & d) Lane-1: Protein ladder (molecular weight markers in kDa), Lane-2: crude enzyme, and Lane-3: purified enzyme. (b) Lane-1: Marker proteins (kDa), Lane-2: purified enzyme, and Lane-3: crude enzyme.

are consistent with earlier studies by Bhaskar et al.¹⁹ on protease and cellulase, Mazhar et al.²⁰ and Lakshmi and Dhandayuthapani²¹ on lipase, and Almanaa et al.²² on amylase production.

After optimization, the maximum yield of 87.5 fold, 42.6 fold, 68.12 fold, and 89.03 fold of protease, lipase, cellulase, and amylase was obtained, respectively, on purification. Homaei and Izadpanah Qeshmi²³ obtained the same findings for protease, Fetyan et al.²⁴ for lipase, and Aladejana et al.²⁵ reported similar results for amylase.

The characterization of purified enzymes was conducted through SDS-PAGE analysis. Results depicted a 29 kDa protein for protease, a 45 kDa protein for lipase and cellulase, and a 56 kDa protein for amylase. Our findings were consistent with previous findings conducted by Demirkhan et al.²⁶.

In the next phase, the purified enzymes were coated with alginate to enhance their efficiency. The characterization of alginate-coated enzymes was done by using FTIR and XRD. The FTIR and XRD analysis confirmed the successful coating of enzymes with alginate. Al-Harbi SA, Almulaiyik²⁷; Mohammadi et al.²⁸, Abdella et al.²⁹, and Wang et al.³⁰ also observed similar peaks for alginate-coated amylase, lipase, protease, and cellulase, respectively. XRD analysis showed sharp peaks indicating a successful crystalline structure of alginate-coated amylase, lipase, protease, and cellulase, which were consistent with a previous study conducted by Khan et al.³¹.

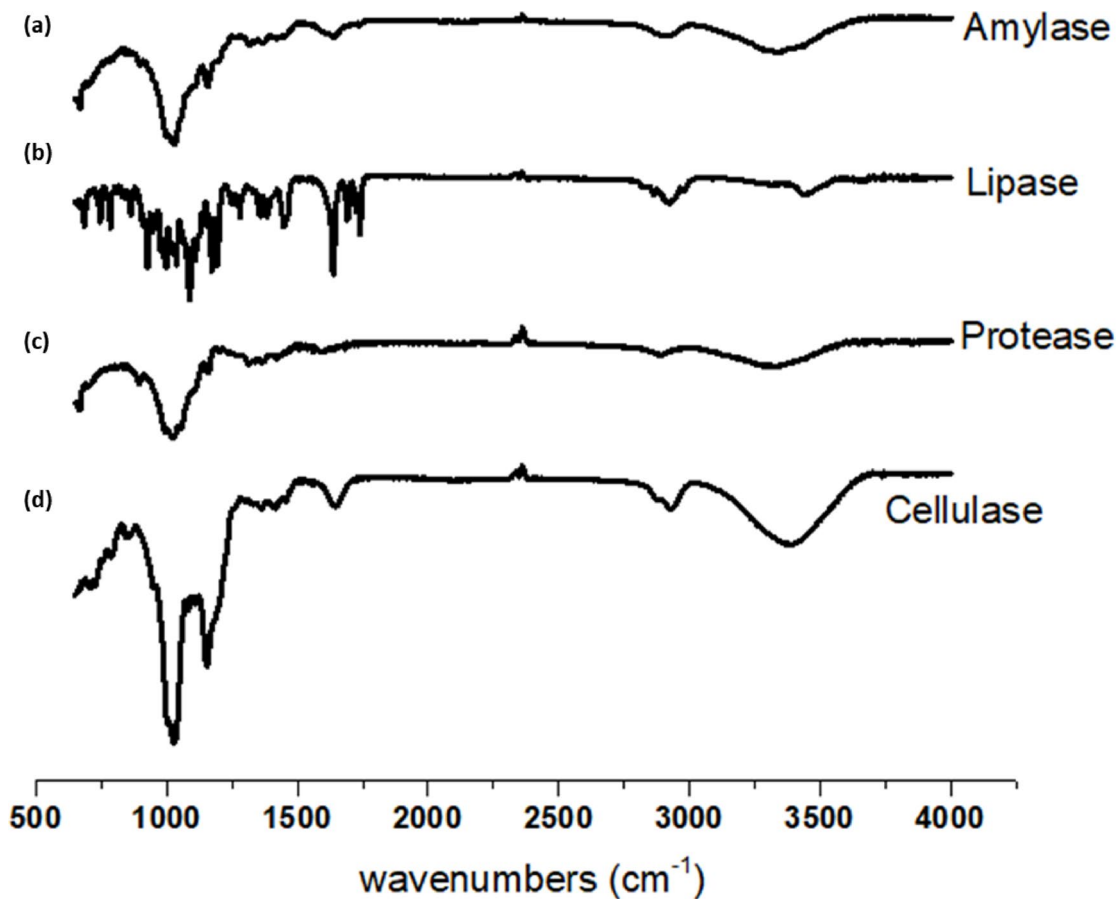


Fig. 6. FTIR analysis of alginate coated (a) amylase, (b) lipase, (c) protease and (d) cellulase.

The alginate-coated enzymes showed an improvement in activities at different pH and temperature ranges than non-coated enzymes. Abd Ellatif³²; Pereira et al.³³ and Çamurlu D, Önal³⁴, reported similar results for optimum pH and temperature ranges for protease, lipase, cellulase, and amylase, respectively.

Alginate encapsulation conferred a consistent protective effect on all enzymes during refrigerated storage. Encapsulated forms retained more than 60% of initial activity after 30 days, whereas the corresponding free enzymes retained only 34–42%. This pattern matches previous reports of encapsulated hydrolases maintaining 60–90% activity after 30–35 days at 4 °C^{49–51}. The alginate matrix likely restricts enzyme mobility, reduces exposure to denaturing factors, and limits autolytic degradation, thereby preserving catalytic function⁵².

Although alginate encapsulation significantly improved stability, other carriers such as chitosan, nanocomposites, and hybrid alginate–polymer systems have been shown to provide even higher retention and reusability. Compared with these advanced carriers, alginate remains advantageous because it is low-cost, food-grade, and simple to apply, making it suitable for feed applications, though with somewhat lower protection compared to nanocomposites.

The enhanced thermostability and pH tolerance of the alginate-encapsulated enzymes indicate potential resilience during feed pelleting and storage, key challenges in enzyme supplementation for poultry diets. These attributes suggest that encapsulation could reduce enzyme degradation before ingestion and improve nutrient digestibility once incorporated into feed. Moreover, the use of a food-grade polymer such as alginate aligns with industrial and regulatory safety requirements. Collectively, these findings provide a foundation for developing a multi-enzyme premix with extended shelf life and improved functionality in poultry feed formulations.

Although the present findings demonstrate promising *in vitro* stability and functional properties, future studies will focus on integrating these enzymes into poultry feed formulations and evaluating growth performance, feed conversion ratio, and nutrient digestibility in broiler trials. Finally, it should be noted that while this study successfully optimized enzyme production, purification, and encapsulation, we did not perform a direct cost-effectiveness study. The reason is that such an analysis requires pilot-scale production data and comparison with commercial enzyme prices, which were beyond the scope of our laboratory-scale work. However, we acknowledge this limitation, and a cost comparison will be included in future scale-up studies.

Conclusion

This study demonstrated that *Bacillus subtilis* is a cost-effective source of protease, lipase, cellulase, and amylase, and that response surface methodology provides efficient optimization of production conditions. Encapsulation

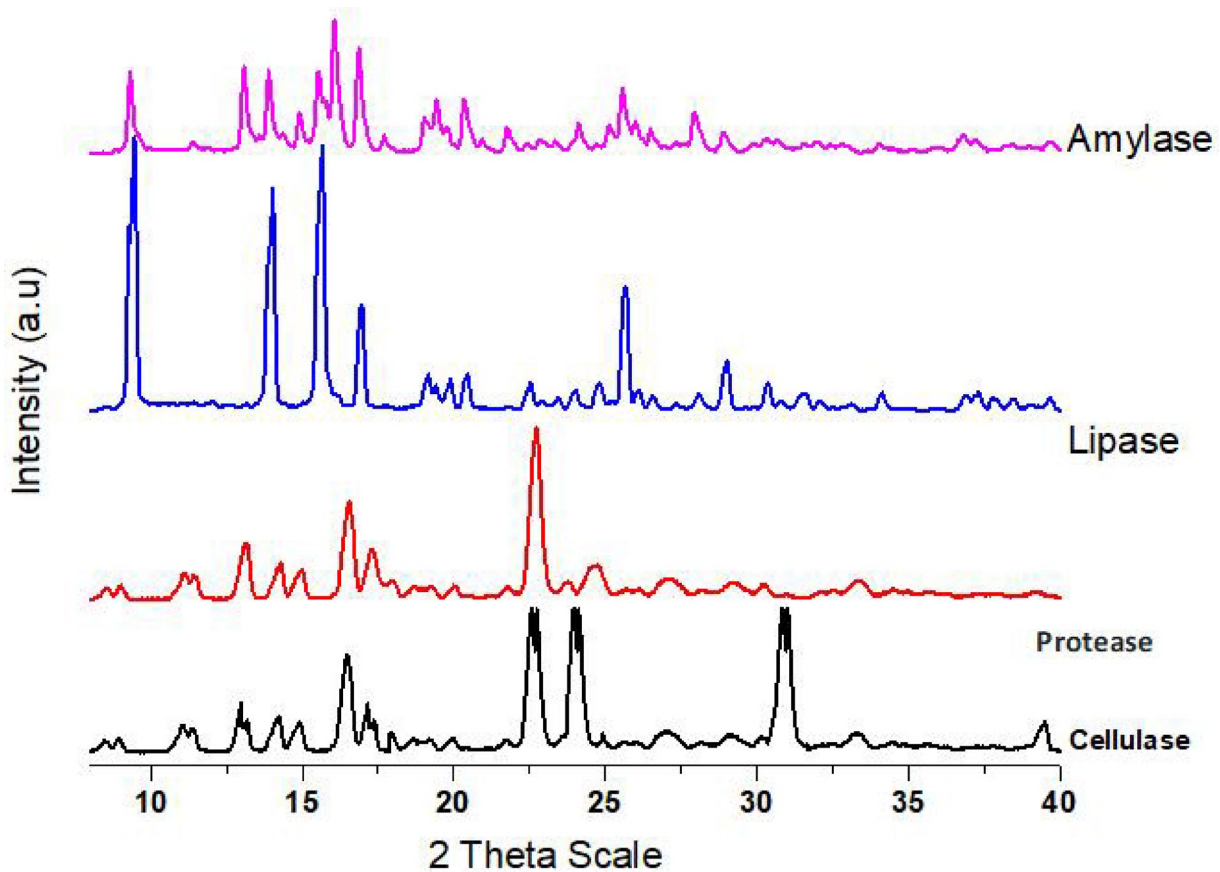


Fig. 7. X-ray Diffraction (XRD) analysis of alginate-coated amylase, lipase, protease, and cellulase.

in alginate beads broadened the active pH and temperature ranges and improved storage stability, with encapsulated enzymes retaining 60–74% activity after 30 days compared to 34–42% for free enzymes. These improvements highlight the potential industrial application of alginate-coated enzymes in poultry feed premixes. However, the absence of *in vivo* feeding trials remains a limitation, and future work will focus on validating enzyme efficacy in poultry systems and comparing costs with commercial enzyme products.

Materials and methods

Materials

All chemicals, unless otherwise specified, were purchased from Sigma-Aldrich (Merck, Darmstadt, Germany). Nutrient broth and agar were obtained from HiMedia Laboratories (Mumbai, India). Sephadex CL-6B was purchased from GE Healthcare (Chicago, IL, USA). Coomassie Brilliant Blue and SDS-PAGE reagents were obtained from Bio-Rad Laboratories (Hercules, CA, USA). Dialysis tubing was from Thermo Fisher Scientific (Waltham, MA, USA). Instruments used included an orbital shaker incubator (Eppendorf, Hamburg, Germany), centrifuge and UV-Vis spectrophotometer (Thermo Fisher Scientific, Waltham, MA, USA), FTIR spectrometer (Bruker, Billerica, MA, USA), and XRD system (PANalytical, Malvern, UK).

Culture Preparation

Bacillus subtilis was used in this current study, and a Pure culture was taken from the Enzyme Biotechnology Laboratory, Department of Biochemistry, University of Agriculture, Faisalabad. The bacteria were cultured in a media described by Mawadza et al.³⁵ with slight modifications. The media contained 2.5 g of tryptone, yeast extract and carboxymethyl cellulose, 0.01 g of nitriloacetic acid, 0.004 g of $\text{CaSO}_4 \cdot \text{H}_2\text{O}$, 0.02 g of $\text{MgCl}_2 \cdot 6\text{H}_2\text{O}$, 1.3 g of ferric citrate and 0.05 mL of $\text{Na}_2\text{HPO}_4 \cdot \text{KH}_2\text{PO}_4$ buffer.

Optimization of fermentation conditions

The substrate wheat straw (5 g) was taken in a 250 mL conical flask, and 5 mL of basal salt was added to the substrate. The optimization of fermentation conditions encompassing pH, temperature, incubation time, and inoculum size for each enzyme was conducted using response surface methodology (RSM). The conditions tested to investigate the maximum yield of each enzyme are depicted in Supplementary Table 1. All the inoculated flasks of fermentation media with carbon and nitrogen source, and all other optimized parameters, 29 runs were applied with the range of fermentation period 24–72 h. After the completion of process, the optimized

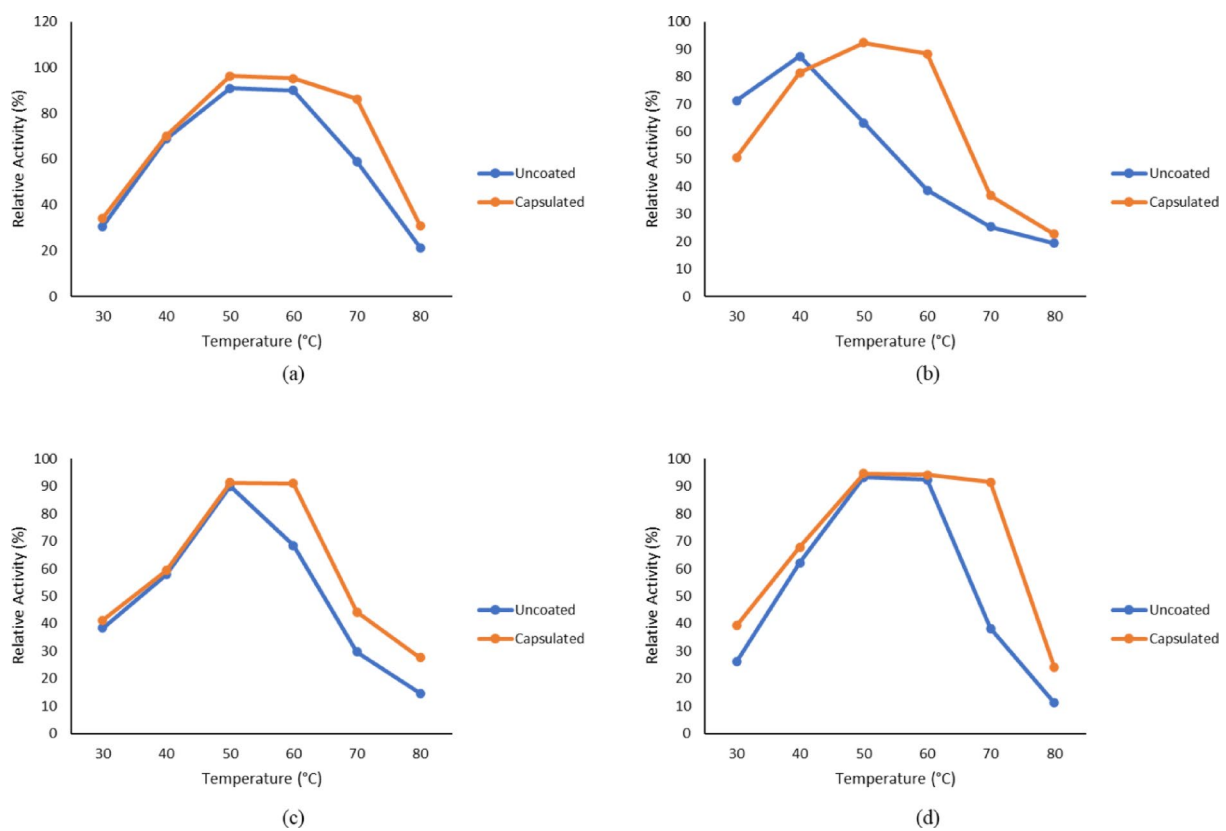


Fig. 8. Effect of temperature on coated and uncoated (a) protease, (b) lipase (c) cellulase and (d) amylase.

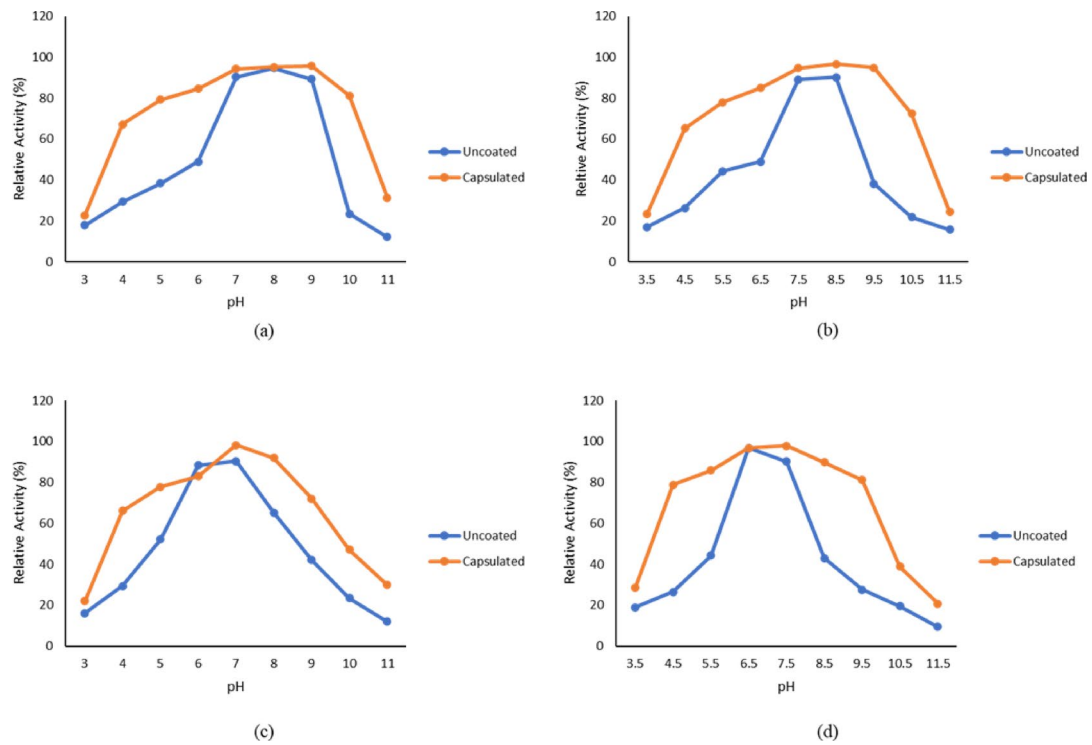


Fig. 9. Effect of pH on coated and uncoated (a) protease, (b) lipase, (c) cellulase and (d) amylase.

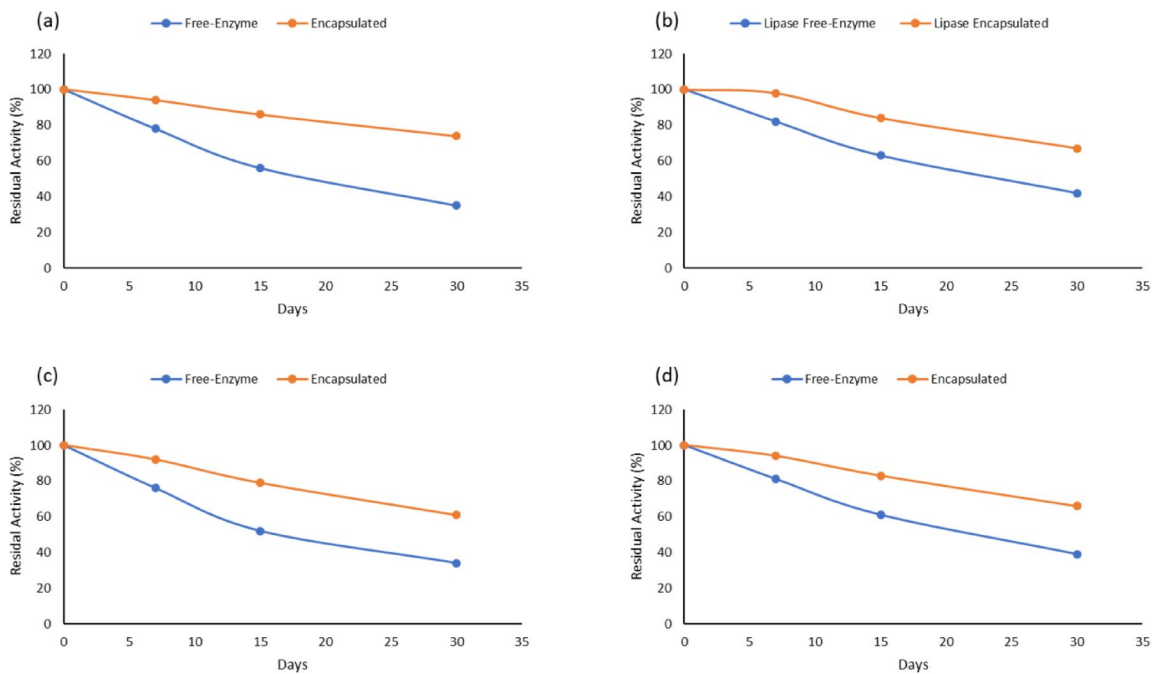


Fig. 10. Stability profile of encapsulated enzymes **(a)** Protease; **(b)** Lipase; **(c)** Cellulase & **(d)** Amylase.

fermentation conditions (pH, temperature, incubation time and inoculum size) were selected for each enzyme at which they give maximum activity³⁶.

After placing the fermentation media in the orbital shaker, all the media were placed in the sterilized Falcon tubes and weighed equally. Then, they were centrifuged at 10,000 rpm for 15 min, and after the centrifugation, we obtained the crude form of the enzyme. The pellets were discarded, and the supernatant is the form of the harvested enzyme³⁷.

Enzyme activity

The protease assay was determined using spectrophotometry. The reaction mixture for the protease assay contains specific chemicals, including casein, tris HCl buffer (pH 8.5), and crude enzyme and incubated for 10 min at 50 °C. After incubation, the reaction was halted by adding 10% TCA. All falcon tubes were placed in ice for one hour. After one hour, the tubes samples underwent filtration and centrifugation at 10,000 rpm for 10 min. The precipitates from the tubes were removed and the absorption was monitored using a spectrophotometer (Thermo Fisher Scientific, USA) at a wavelength of 280 nm³⁸.

For lipase activity, the reaction mixture contained Arabic gum, a 0.2 M phosphate buffer with a pH of 7, and coconut oil, combined in a 2:1:1 ratio. These components were thoroughly mixed to ensure a homogeneous solution. An aliquot of 0.1 mL of this prepared substrate solution was transferred to a flask, to which 1 mL of a 1 M CaCl₂ solution was added. Subsequently, 0.01 mL of crude enzyme was introduced, and the mixture was incubated on a rotary agitator at 30 °C for 1 h, at a rotational speed of 150 rpm. After the incubation period, the reaction was terminated by the addition of 5 mL of a 1:1 acetone-ethanol mixture, and the solution was stirred thoroughly. The resulting mixture was then titrated with 0.01 N NaOH until a distinct color change to pink was observed³⁹.

For cellulase activity, the enzyme was introduced to test tubes with a capacity of 0.5 mL. Each test tube included a paper strip measuring 1 × 6 cm, along with 1 mL of a NaAc buffer with a concentration of 50 mM and a pH of 4.8. Following a 60-minute incubation in a water bath set at 50 °C, 3 mL of DNS reagent was introduced into each tube, which was then subjected to vigorous boiling for a duration of 5 min. After diluting the colored solution with 20 mL of H₂O, 200 µL samples were transferred to a 96-well flat bottom plate (Corning, NY). The absorbance at 540 nm was then measured using a plate reader (Bio-TEK, Power Wave HT model, Winooski, Vermont)⁴⁰.

The amylase activity was measured using the 3,5-Dinitrosalicylic Acid (DNS) method as described by Msarah et al.⁴¹. Specifically, 0.5 mL of each enzyme source was combined with 1% soluble starch, which had been dissolved in a 0.1 M phosphate buffer at pH 7. This mixture was incubated at 55 °C for 15 min. To halt the reaction, 1 ml of DNS reagent was introduced. The resulting mixture was then boiled for 10 min. Following boiling, distilled water was added to adjust the total volume to 12 mL. The concentration of reducing sugars produced was determined by measuring absorbance at 540 nm.

Enzyme purification

Ammonium sulphate precipitation

The partial purification of enzymes was performed by using ammonium sulphate (Sigma-Aldrich, Germany) precipitation method. Firstly, the saturation point for Amylase was found which is 70% (70 g of $(\text{NH}_3)_2\text{SO}_4$ in 100mL) then further process was proceed. In which, two steps were followed to attain purified enzyme⁴⁷.

Dialysis

The obtained pellets of the enzymes were placed in dialysis bag and close from both sides tightly and placed in the 0.1 M phosphate buffer beaker stirred on magnetic stirrer for at least 4 h process shown in Fig. 3.4. After that, the purified enzymes were shifted in Eppendorf for further enzyme assays and protein content, along with other purification step⁴¹.

Gel filtration

After dialysis, enzyme samples were further purified by gel filtration chromatography following the method of Dhayalan et al⁴³, with modifications. Sephadex CL-6B (GE Healthcare, Chicago, IL, USA) was swollen in distilled water and heated at 96 °C for 5–6 h before packing into the column. The column was equilibrated with 0.1 M phosphate buffer. A 0.5 mL aliquot of the most active ion-exchange fraction was loaded, and 50 fractions (2 mL each) were collected at a constant flow rate using phosphate buffer. Enzyme activity and protein content were measured in each fraction to identify the peak fractions.

Characterization of enzymes

Protease, lipase, cellulase, and amylase were characterized by SDS-PAGE following the method of Fincan et al⁴⁴, with minor modifications. A 5% stacking gel and 12% resolving gel were prepared. Purified enzyme samples were mixed 1:1 with sample buffer, vortexed briefly, and heated at 95 °C for 3–4 min. Approximately 10–14 μL of each sample, along with protein markers, was loaded onto the gel. Electrophoresis was performed at 80 V until the dye front reached the bottom.

Gels were stained with Coomassie Brilliant Blue ((Hercules, CA, USA) for 2 h with gentle shaking, rinsed with distilled water, and destained with destaining solution until protein bands became visible.

Enzyme encapsulation

The extrusion method was used to encapsulate enzymes. The enzymes were coated using the alginate standard technique, as described by Qamar et al.⁴⁵. Each enzyme was individually introduced into a hydrocolloid solution called alginate. Subsequently, the cell suspension was forced through a syringe needle to create droplets. These droplets were then allowed to fall freely into a bath containing a solution called CaCl_2 , which causes them to harden. The alginate concentration used was 1% in order to create a gel with a CaCl_2 concentration of 0.5 M. The experimental diets were supplemented with enzymes coated with alginate to ensure uniformity in the size and shape of the beads.

Encapsulation was performed using the purified enzyme fraction with the highest specific activity obtained after gel filtration (Table 1). This approach ensured that each alginate bead contained the maximum amount of active enzyme and allowed a direct comparison of activity before and after encapsulation.

Characterization of encapsulated enzymes

FTIR analysis To perform FTIR spectroscopy on alginate-coated enzymes, the samples were first prepared by grinding them into a fine powder if solid or diluting them if liquid. A small amount of the powdered sample or a drop of the liquid sample was placed onto the FTIR sample holder, either as a potassium bromide (KBr) pellet or using an attenuated total reflectance (ATR) accessory. For KBr, the sample was mixed with KBr and pressed into a thin pellet, whereas for ATR, the sample was placed directly on the crystal surface. The FTIR instrument (Billerica, MA, USA) was calibrated according to the manufacturer's instructions. The spectral scan was conducted over a range of 4000 to 400 cm^{-1} with a resolution of 4 cm^{-1} to capture the infrared absorbance⁴⁶.

XRD analysis

To perform X-ray diffraction (XRD) analysis on alginate-coated enzymes, the samples were prepared by grinding them into a fine powder. The powdered sample was then placed into the sample holder of the X-ray diffractometer (Malvern, UK). The X-ray source was set to use $\text{Cu K}\alpha$ radiation ($\lambda = 1.5418 \text{ \AA}$), and the scan was conducted over a 2θ range from 5° to 70°, with a step size of 0.02° and a scan speed of 2°/min. The resulting XRD pattern was examined for multiple diffraction peaks, which indicated well-defined crystalline structures⁴⁷.

Enzyme kinetics

Effect of temperature

The purified enzymes and encapsulated enzymes were incubated with substrate at different temperature ranges (30–80 °C)⁴⁵.

Effect of pH

The purified enzymes and encapsulated enzymes were incubated with substrate at different pH ranges⁴⁵. For protease and cellulase, pH ranges were selected from 3 to 11, and for lipase and amylase, the selected pH ranges were between 3.5 and 11.5.

Storage stability

Free and encapsulated enzyme samples with equal initial activity were stored at 4 °C. Residual activity was determined after 0, 7, 15 and 30 days. Encapsulated samples were dissolved in sodium citrate buffer before assay. Residual activity was expressed as percentage of the day-0 activity.

Statistical analysis

All biological assays were performed in triplicate ($n=3$) and data are reported as mean \pm standard deviation (SD). Response surface methodology (RSM) was implemented using a central composite design (CCD) with 29 runs using Design-Expert v.12 (or specify software used). Four independent variables (pH, temperature, incubation time, and inoculum size) were optimized to maximize enzyme production. Analysis of variance (ANOVA) was used to test model significance and lack-of-fit. Model adequacy was evaluated using R^2 , adjusted R^2 , predicted R^2 and residual analysis. Statistical significance was accepted at $p < 0.05$ ⁴⁸.

Data availability

All data generated or analyzed during this study are included in this published article and its supplementary information files.

Received: 20 July 2025; Accepted: 11 December 2025

Published online: 20 December 2025

References

1. Deckers, M., Deforce, D., Fraiture, M. A. & Roosens, N. H. Genetically modified micro-organisms for industrial food enzyme production: an overview. *Foods* **9**, 326 (2020).
2. Verduzco-Oliva, R. & Gutierrez-Uribe, J. A. Beyond enzyme production: solid state fermentation (SSF) as an alternative approach to produce antioxidant polysaccharides. *Sustainability* **12**, 495 (2020).
3. Wang, P., Peng, C., Xie, X., Deng, X. & Weng, M. Research progress on the fibrinolytic enzymes produced from traditional fermented foods. *Food Sci. Nutr.* **11**, 5675–5688 (2023).
4. Ding, Q. & Ye, C. Microbial cell factories based on filamentous bacteria, yeasts, and fungi. *Microb. Cell. Fact.* **22**, 20 (2023).
5. Patel, A. K., Dong, C. D., Chen, C. W., Pandey, A. & Singhania, R. R. in *Biotechnology of microbial enzymes* 25–57Elsevier, (2023).
6. Akinsemolu, A. A., Onyeaka, H., Odion, S. & Adebanjo, I. Exploring *Bacillus subtilis*: Ecology, biotechnological applications, and future prospects. *J. Basic Microbiol.* **64**, 2300614 (2024).
7. Liu, X. & Kokare, C. in *Biotechnology of microbial enzymes* 405–444 (Elsevier, 2023).
8. Shi, H. et al. *Bacillus subtilis* field spray on alpine meadows promotes digestibility in Tibetan sheep via increasing the nutrient quality of herbage and enhancing rumen bacterial populations. *Anim. Feed Sci. Technol.* **310**, 115920 (2024).
9. Bontà, V. et al. An in vitro study on the role of cellulases and Xylanases of *Bacillus subtilis* in dairy cattle nutrition. *Microorganisms* **12**, 300 (2024).
10. Bhattacharya, R., Arora, S. & Ghosh, S. Bioprocess optimization for food-grade cellulolytic enzyme production from sorghum waste in a novel solid-state fermentation bioreactor for enhanced Apple juice clarification. *J. Environ. Manage.* **358**, 120781 (2024).
11. Thirunavukkarasu, M., Sawle, Y. & Lala, H. A comprehensive review on optimization of hybrid renewable energy systems using various optimization techniques. *Renew. Sustain. Energy Rev.* **176**, 113192 (2023).
12. Abdollahzadeh, R., Pazhang, M., Najavand, S., Fallahzadeh-Mamaghani, V. & Amani-Ghadim, A. R. Screening of pectinase-producing bacteria from farmlands and optimization of enzyme production from selected strain by RSM. *Folia Microbiol.* **65**, 705–719 (2020).
13. Pereira, L. M. S., Milan, T. M. & Tapia-Blácido, D. R. Using response surface methodology (RSM) to optimize 2G bioethanol production: A review. *Biomass Bioenerg.* **151**, 106166 (2021).
14. Kumar, N., Sharma, R., Saharan, V., Yadav, A. & Aggarwal, N. K. Enhanced xylanolytic enzyme production from *parthenium hysterophorus* through assessment of the RSM tool and their application in saccharification of lignocellulosic biomass. *3 Biotech.* **13**, 396 (2023).
15. Li, Z., Zheng, M., Zheng, J. & Gänzle, M. G. *Bacillus* species in food fermentations: an underappreciated group of organisms for safe use in food fermentations. *Curr. Opin. Food Sci.* **50**, 101007 (2023).
16. ayak, S. K. Multifaceted applications of probiotic *Bacillus* species in aquaculture with special reference to *Bacillus subtilis*. *Reviews Aquaculture* **13**, 862–906 (2021).
17. Su, Y., Liu, C., Fang, H. & Zhang, D. *Bacillus subtilis*: a universal cell factory for industry, agriculture, biomaterials and medicine. *Microb. Cell. Fact.* **19**, 173 (2020).
18. Yadav, A. et al. Enhanced co-production of pectinase, cellulase and Xylanase enzymes from *Bacillus subtilis* ABDR01 upon ultrasonic irradiation. *Process Biochem.* **92**, 197–201 (2020).
19. Bhaskar, N., Sudeepa, E., Rashmi, H. & Selvi, A. T. Partial purification and characterization of protease of *Bacillus proteolyticus* CFR3001 isolated from fish processing waste and its antibacterial activities. *Bioresour. Technol.* **98**, 2758–2764 (2007).
20. Mazhar, H. et al. Optimized production of lipase from *Bacillus subtilis* PCSIRNL-39. *Afr. J. Biotechnol.* **16**, 1106–1115 (2017).
21. Lakshmi, D. & Dhandayuthapani, K. Statistical Optimization of Lipase Production From Mutagenic Strain of Newly Isolated *Bacillus licheniformis* MLP. *Mapana J. Sciences* **21**, (2022).
22. Almanaa, T. N. et al. Solid state fermentation of amylase production from *Bacillus subtilis* D19 using agro-residues. *J. King Saud University-Science* **32**, 1555–1561 (2020).
23. Homaei, A. & Izadpanah Qeshmi, F. Purification and characterization of a robust thermostable protease isolated from *Bacillus subtilis* strain HR02 as an extremozyme. *J. Appl. Microbiol.* **133**, 2779–2789 (2022).
24. Fetyan, N. H., Ismail, I. M., Reda, S., Mohamed, A. M. & Isolation Purification, and production of lipase from *Bacillus subtilis* isolated from food processing wastes and its application in biodiesel production. *Egypt. J. Chem.* **66**, 173–187 (2023).
25. Aladejana, O. M., Oyedele, O., Omoboye, O. & Bakare, M. Production, purification and characterization of thermostable alpha amylase from *Bacillus subtilis* Y25 isolated from decaying Yam (*Dioscorea rotundata*) tuber. *Notulae Scientia Biologicae* **12**, 154–171 (2020).
26. Demirkhan, E., Çetinkaya, A. A. & Abdou, M. Lipase from new isolate *Bacillus cereus* ATA179: optimization of production conditions, partial purification, characterization and its potential in the detergent industry. *Turkish J. Biology* **45**, 287–300 (2021).
27. Al-Harbi, S. A. & Almulaiqa, Y. Q. Purification and biochemical characterization of Arabian Balsam α -amylase and enhancing the retention and reusability via encapsulation onto calcium alginate/Fe2O3 nanocomposite beads. *Int. J. Biol. Macromol.* **160**, 944–952 (2020).

28. Mohammadi, N. S., Khiabani, M. S., Ghanbarzadeh, B. & Mokarram, R. R. Enhancement of biochemical aspects of lipase adsorbed on Halloysite nanotubes and entrapped in a Polyvinyl alcohol/alginate hydrogel: strategies to reuse the most stable lipase. *World J. Microbiol. Biotechnol.* **36**, 45 (2020).
29. Abdella, M. A., Ahmed, S. A. & Hassan, M. E. Protease immobilization on a novel activated carrier alginate/dextrose beads: improved stability and catalytic activity via covalent binding. *Int. J. Biol. Macromol.* **230**, 123139 (2023).
30. Wang, Y. et al. Cellulase immobilized by sodium alginate-polyethylene glycol-chitosan for hydrolysis enhancement of microcrystalline cellulose. *Process Biochem.* **107**, 38–47 (2021).
31. Khan, H. et al. Experimental methods in chemical engineering: X-ray diffraction spectroscopy—XRD. *Can. J. Chem. Eng.* **98**, 1255–1266 (2020).
32. Abd Ellatif, S., ENCAPSULATION OF PROTEASE & ENZYME FOR DOMESTIC APPLICATION. *Al-Azhar J. Pharm. Sci.* **61**, 117–133 (2020).
33. Pereira, A. et al. d. S. Chitosan-alginate beads as encapsulating agents for *Yarrowia lipolytica* lipase: Morphological, physico-chemical and kinetic characteristics. *International journal of biological macromolecules* **139**, 621–630 (2019).
34. Çamurlu, D. & Önal, S. Encapsulation and characterization of cellulase purified with three-phase partitioning technique. *Biocatal. Biotransform.* **39**, 292–301 (2021).
35. Mawadza, C., Hatti-Kaul, R., Zvauya, R. & Mattiasson, B. Purification and characterization of cellulases produced by two *Bacillus* strains. *J. Biotechnol.* **83**, 177–187 (2000).
36. Jujjavarapu, S. E. & Dhagat, S. Evolutionary trends in industrial production of α -amylase. *Recent Patents Biotechnol.* **13**, 4–18 (2019).
37. Danilova, I. & Sharipova, M. The practical potential of bacilli and their enzymes for industrial production. *Front. Microbiol.* **11**, 1782 (2020).
38. Leite, J. A. et al. Heat-treatments affect protease activities and peptide profiles of ruminants' milk. *Front. Nutr.* **8**, 626475 (2021).
39. Yasar, G., Gulhan, U. G., Guduk, E. & Aktas, F. Screening, partial purification and characterization of the hyper-thermophilic lipase produced by a new isolate of *Bacillus subtilis* LP2. *Biocatal. Biotransform.* **38**, 367–375 (2020).
40. Malik, W. A. & Javed, S. Biochemical characterization of cellulase from *Bacillus subtilis* strain and its effect on digestibility and structural modifications of lignocellulose rich biomass. *Front. Bioeng. Biotechnol.* **9**, 800265 (2021).
41. Msarah, M. J., Ibrahim, I., Hamid, A. A. & Aqma, W. S. Optimisation and production of alpha amylase from thermophilic *Bacillus* spp. and its application in food waste biodegradation. *Helijon* **6**, (2020).
42. Illuri, R. et al. Production, partial purification and characterization of ligninolytic enzymes from selected basidiomycetes mushroom fungi. *Saudi J. Biol. Sci.* **28**, 7207–7218 (2021).
43. Dhayalan, A. et al. Isolation of a bacterial strain from the gut of the fish, *systemus sarana*, identification of the isolated strain, optimized production of its protease, the enzyme purification, and partial structural characterization. *J. Genetic Eng. Biotechnol.* **20**, 24 (2022).
44. Fincan, S. A. et al. Purification and characterization of thermostable α -amylase produced from *Bacillus licheniformis* So-B3 and its potential in hydrolyzing Raw starch. *Life Sci.* **264**, 118639 (2021).
45. Qamar, S. A., Asgher, M. & Bilal, M. Immobilization of alkaline protease from *Bacillus brevis* using Ca-alginate entrapment strategy for improved catalytic stability, silver recovery, and dehairing potentialities. *Catal. Lett.* **150**, 3572–3583 (2020).
46. Rathore, C. et al. Standardization of micro-FTIR methods and applicability for the detection and identification of microplastics in environmental matrices. *Sci. Total Environ.* **888**, 164157 (2023).
47. Ali, A., Chiang, Y. W. & Santos, R. M. X-ray diffraction techniques for mineral characterization: A review for engineers of the fundamentals, applications, and research directions. *Minerals* **12**, 205 (2022).
48. Priyadharsini, P. & Dawn, S. Optimization of fermentation conditions using response surface methodology (RSM) with kinetic studies for the production of bioethanol from rejects of *Kappaphycus Alvarezii* and solid food waste. *Biomass Convers. Biorefinery.* **13**, 9977–9995 (2023).
49. Vasilescu, C., Marc, S., Hulk, I. & Paul, C. Enhancement of the catalytic performance and operational stability of sol-gel-entrapped cellulase by tailoring the matrix structure and properties. *Gels* **8**, 626 (2022).
50. Yandri, Y. et al. The Stability Improvement of α -Amylase Enzyme from *Aspergillus fumigatus* by Immobilization on a Bentonite Matrix. *Biochemistry research international* **3797629** (2022). (2022).
51. Yao, Z., Li, Y. & Xu, W. Micro-immobilized enzyme reactors for mass spectrometry proteomics. *Analyst* **150**, 3000–3010 (2025).
52. Hertzberg, S., Kvittingen, L., Anthonsen, T. & Skjaak-Braek, G. Alginate as immobilization matrix and stabilizing agent in a two-phase liquid system: application in lipase-catalysed reactions. *Enzym. Microb. Technol.* **14**, 42–47 (1992).

Author contributions

Hamza Rafeeq has prepared the whole manuscript. Muhammad Anjum Zia, Muhammad Shahid and Muhammad Sarwar Khan supervised Hamza Rafeeq to prepare this manuscript.

Declarations

Competing interests

The authors declare no competing interests.

Additional information

Supplementary Information The online version contains supplementary material available at <https://doi.org/10.1038/s41598-025-32668-6>.

Correspondence and requests for materials should be addressed to H.R. or M.A.Z.

Reprints and permissions information is available at www.nature.com/reprints.

Publisher's note Springer Nature remains neutral with regard to jurisdictional claims in published maps and institutional affiliations.

Open Access This article is licensed under a Creative Commons Attribution-NonCommercial-NoDerivatives 4.0 International License, which permits any non-commercial use, sharing, distribution and reproduction in any medium or format, as long as you give appropriate credit to the original author(s) and the source, provide a link to the Creative Commons licence, and indicate if you modified the licensed material. You do not have permission under this licence to share adapted material derived from this article or parts of it. The images or other third party material in this article are included in the article's Creative Commons licence, unless indicated otherwise in a credit line to the material. If material is not included in the article's Creative Commons licence and your intended use is not permitted by statutory regulation or exceeds the permitted use, you will need to obtain permission directly from the copyright holder. To view a copy of this licence, visit <http://creativecommons.org/licenses/by-nc-nd/4.0/>.

© The Author(s) 2025